Exploration of Physical Principles Underlying Lipid Regular Distribution: Effects of Pressure, Temperature, and Radius of Curvature on E/M Dips in Pyrene-labeled PC/DMPC Binary Mixtures

Parkson Lee-Gau Chong,* Daxin Tang,* and Istvan P. Sugar‡

*Department of Biochemistry, Temple University School of Medicine, Philadelphia, Pennsylvania 19140; Department of Biochemistry, Meharry Medical College, Nashville, Tennessee 37208; and ‡Department of Biomathematical Sciences and Physiology and Biophysics, The Mount Sinai Medical Center, New York, New York 10029 USA

ABSTRACT In a previous study, we observed a series of dips in the plot of E/M (the ratio of excimer to monomer fluorescence intensity) versus the mole fraction of 1-palmitoyl-2-(10-pyrenyl)decanoyl-*sn*-glycerol-3-phosphatidylcholine (Pyr-PC) in Pyr-PC/DMPC binary mixtures at 30°C. In the present study, we have characterized the physical nature of E/M dips in Pyr-PC/DMPC binary mixtures by varying pressure, temperature, and vesicle diameter. The E/M dips at 66.7 and at 71.4 mol% PyrPC in DMPC multilamellar vesicles remain discernible at 30–43°C. At higher temperatures (e.g., 53°C), the depth of the dip abruptly becomes smaller. This result agrees with the idea that E/M dips appear as a result of regular distribution of pyrene-labeled acyl chains into hexagonal super-lattices at critical mole fractions. Regular distribution is a self-ordering phenomenon. Usually, in self-ordered systems, the number of structural defects increases with increasing temperature, and thermal fluctuations eventually result in an order-to-disorder transition. The effect of vesicle diameter on the E/M dip at 66.7 mol% Pyr-PC in DMPC has been studied at 37.5°C by using unilamellar vesicles of varying sizes. The E/M dip is observable in large unilamellar vesicles; however, the depth of the E/M dip decreases when the vesicle diameter is reduced. When the vesicle diameter is reduced to about 64 nm, the dip becomes shallow and split. This result suggests that the curvature-induced increase in the separation of lipids in the outer monolayer decreases the tendency of regular distribution for pyrene-labeled acyl chains. Regular distribution is believed to arise from the long-range repulsive interaction between Pyr-PC molecules due to the elastic deformation of the lipid matrix around the bulky pyrene moiety. When the radius of curvature becomes small, outer monolayer lipids are more separated. Therefore, pyrene-containing acyl chains fit better into the membrane matrix, which alleviates the deformation of the lattice and diminishes the long-range repulsive interactions between pyrene-containing acyl chains. Furthermore, we have shown a striking difference in the pressure dependence of E/M at critical Pyr-PC mole fractions and at noncritical mole fractions. In the pressure range between 0.001 and 0.7 kbar at 30°C, E/M decreases steadily with increasing pressure at noncritical mole fractions; in contrast, E/M changes little with pressure at critical mole fractions (e.g., 33.3 and 50.0 mol% Pyr-PC). The pressure data suggest that membrane free volume in the liquid crystalline state of the bilayer is less abundant at critical Pyr-PC mole fractions than at noncritical mole fractions.

INTRODUCTION

In theory, lipids in two-component membranes can be laterally organized in three ways: domain separation, random distribution, and regular distribution (Von Dreele, 1978). A regular distribution is a lateral organization where the guest molecules are maximally separated in the lipid matrix. Although examples of lipid random distribution and domain formation are voluminous in the literature, few studies have reported lipid regular distribution.

The first experimental evidence for lipid regular distribution was reported by Somerharju et al. (1985). Using the fluorescence of 1-palmitoyl-2-(10-pyrenyl)decanoyl-*sn*-glycerol-3-phosphatidylcholine (Pyr-PC) in egg yolk phosphatidylcholine and in L-α-dipalmitoylphosphatidylcholine (DPPC), they showed that the plot of the ratio of the excimer to monomer fluorescence intensity (E/M) versus the mole fraction of Pyr-PC, X_{PyrPC}, has several linear regions separated by kinks. The appearance of the E/M kinks has been interpreted in terms of the regular distribution of Pyr-PC into hexagonal super-lattices (Somerharju et al., 1985; Mustonen et al., 1987; Virtanen et al., 1988). The hexagonal super-lattice model proposes that (1) the acyl chains of the phospholipids form a hexagonal host lattice, (2) pyrene-containing acyl chains are guest elements, which are bulky, causing steric perturbation in the host lattice, and (3) the guest elements tend to be maximally separated to minimize the total energy. According to Ruocco and Shipley (1982), the acyl chains of phospholipids can be arranged into a quasi two-dimensional hexagonal lattice, as illustrated in Fig. 1, in

Received for publication 2 February 1994 and in final form 28 March 1994.

Address reprint requests to Parkson Lee-Gau Chong, Department of Biochemistry, Temple University School of Medicine, 3420 North Broad Street, Philadelphia, PA 19140. Tel.: 215-707-4182; Fax: 215-707-7536.

Abbreviations used: DMPC, L-α-dimyristoylphosphatidylcholine; DPPC, L-α-dipalmitoylphosphatidylcholine; MLV, multilamellar vesicles; LUV, large unilamellar vesicles; Pyr-PC, 1-palmitoyl-2-(10-pyrenyl)decanoyl-*sn*-glycerol-3-phosphatidylcholine; T_m, main phase transition temperature; X_{PyrPC}, mole fraction of Pyr-PC in DMPC; Y'_{PyrPC}, critical mole fraction of Pyr-PC at which the acyl chains of DMPC form regularly distributed hexagonal super-lattices; Y_{PyrPC}, critical mole fraction of Pyr-PC at which the pyrene-containing acyl chains form regularly distributed hexagonal super-lattices; Z, the ratio of regular areas to irregular areas.

0006-3495/94/06/2029/10 $2.00

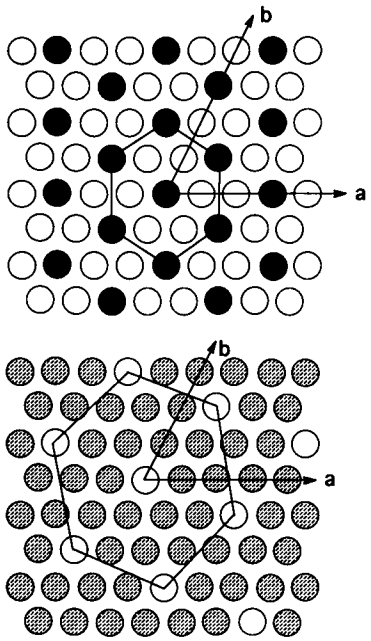

FIGURE 1 (*Top*) Schematic diagram for the regular distribution pattern of 66.7 mol% Pyr-PC in DMPC. The dark circles are pyrene-containing acyl chains, whereas the open circles are unlabeled acyl chains. (*Bottom*) The regular pattern for 71.4 mol% Pyr-PC in DMPC. The open circles are the DMPC acyl chains participating in the hexagonal super-lattices, and the dashed circles are either the pyrene-containing acyl chains or the unlabeled chains not participating in the super-lattices (Tang and Chong, 1992).

which the dark circles are the acyl chains containing the pyrene moiety and the open circles represent the unlabeled acyl chains. For a given acyl chain, its position can be described by two coordinates once the origin and the principal axes have been defined. Thus, the lateral position of a dark circle in Fig. 1 (*top*) can be described by a coordinate (n_a, n_b) where n_a and n_b are the number of translational steps in the lattice along the two principal axes a and b, respectively. In the regular distribution, Pyr-PC molecules may establish a hexagonal super-lattice within the host lattice. The critical Pyr-PC mole fraction, $Y_{PyrPC}(n_a, n_b)$, for the pyrene-containing acyl chains to form the regularly distributed hexagonal super-lattices can be calculated by the equation (Kinnunen et al., 1987; Virtanen et al., 1988)

$$Y_{PyrPC}(n_a, n_b) = 2/(n_a^2 + n_a n_b + n_b^2). \quad (1)$$

Although the E/M kinks observed by Somerharju et al. (1985) seem to agree with Eq. 1, only a few E/M kinks were observed.

Recently, we reinvestigated this problem by monitoring the E/M value of Pyr-PC in L-α-dimyristoylphosphatidylcholine (DMPC) multilamellar vesicles (MLV) at much smaller mole fraction intervals over a wide range of concentrations (up to almost 100 mol% Pyr-PC). We observed a series of dips, in addition to kinks, in the plot of E/M versus X_{PyrPC} in Pyr-PC/DMPC binary mixtures at 30°C (Tang and Chong, 1992).

The E/M dips were interpreted in terms of the extended hexagonal super-lattice model (Tang and Chong, 1992). According to this model, the E/M dips/kinks below 66.7 mol% Pyr-PC (excluding the dip/kink at 33.3 mol%) were formed as a result of the pyrene-containing acyl chains being regularly distributed in the DMPC lipid matrix. The dip positions in this concentration region agree with Eq. 1. On the other hand, the dips above 66.7 mol% plus the dip/kink at 33.3 mol% can be described by Eq. 2 (Tang and Chong, 1992) as

$$Y'_{PyrPC}(m_a, m_b) = 1 - (2/(m_a^2 + m_a m_b + m_b^2)) \quad (2)$$

where Y'_{PyrPC} is the critical mole fraction of Pyr-PC at which the acyl chains of DMPC form regularly distributed hexagonal super-lattices and m_a and m_b are the projections along the axis a and b, respectively, for an acyl chain of DMPC in the super-lattice (Fig. 1, *bottom*). This interpretation is based on the idea that if Pyr-PC is regularly distributed into super-lattices in the DMPC matrix at Y_{PyrPC} when Pyr-PC is the minor component, then DMPC should be regularly distributed into super-lattices in the Pyr-PC matrix at $(1 - Y_{PyrPC})$ when DMPC is the minor component. The good agreement between the observed dips and the Y or Y' values predicted from Eqs. 1 and 2 provides strong evidence that lipids in the Pyr-PC/DMPC binary mixtures are regularly distributed at 30°C (Tang and Chong, 1992).

Since the observation of E/M dips, some physical properties pertaining to lipid regular distribution in Pyr-PC/DMPC mixtures have been proposed. First, as implicated by the third law of thermodynamics, a perfect super-lattice arrangement through the entire membrane can occur only at absolute zero temperature. Therefore, imperfect super-lattices due to thermal fluctuations, impurities, and/or variations in membrane curvature are expected to occur under ambient conditions. The coexistence of regular regions with irregular regions has been used to explain why E/M does not go to zero at critical Pyr-PC mole fractions (Tang and Chong, 1992). This idea has been corroborated by computer simulations (Sugar et al., 1993 and 1994) that further indicate that the ratio of regular areas (where regular patterns can be recognized from the snapshot of simulated lateral distributions) to irregular areas (where regular patterns cannot be recognized) reaches a local maximum at a critical mole fraction and a minimum between two neighboring critical mole fractions. Membrane defect or void space is more likely to occur in the irregular region because a regular region requires a more stringent structural arrangement. This consideration, taken together with the results of computer simulations, strongly implies that membrane free volume in Pyr-PC/DMPC mixtures is less at critical mole fractions and more between two neighboring critical mole fractions.

Second, molecular dynamics simulations indicate that the deformation in the hexagonal lattice caused by the bulky pyrene ring generates a long-range repulsive interaction between pyrene-containing acyl chains (J. A. Virtanen, unpublished results). This long-range repulsion is believed to be the main physical origin for the maximal separation of Pyr-PC molecules in the membrane, which leads to the drop of the E/M value at critical mole fractions. When the separation of matrix lipids increases, the pyrene-containing acyl chains are

able to fit better into the membrane lattice, which alleviates the deformation of the lattice and diminishes the long-range repulsive interactions. This suggests that the E/M dip should vary with the intermolecular distance between matrix lipids. Third, it has been proposed that the appearance of an E/M dip requires a fine balance between the energy minimization due to maximal separation of the bulky pyrene rings in the membrane and the entropy-driven randomization (Tang and Chong, 1992). Maximal separation of pyrene-containing acyl chains into hexagonal super-lattices is a behavior of self-ordering. Usually, the number of structural defects in self-ordered systems increases with increasing temperature, and thermal fluctuations eventually lead to an order-to-disorder transition (Haken, 1983). This immediately suggests that E/M dips will diminish at high temperatures where entropy-driven randomization prevails.

In the present study, the above proposed physical properties have been tested via the studies of E/M dips as a function of pressure, temperature, and vesicle diameter. The obtained results are consistent with theoretical predictions and reveal certain fundamental physical principles underlying lipid regular distribution in membranes.

MATERIALS AND METHODS

Materials

Pyr-PC obtained from Molecular Probes (Eugene, OR) was purified by high-performance liquid chromatography with a C-18 reverse-phase column (3.9x150 mm, μ-Bondapak, Millipore, Marlboro, MA) using methanol/acetonitrile (67:33, v/v) as the mobile phase. DMPC was purchased from Avanti Polar Lipids (Alabaster, AL) and used as such. The concentration of Pyr-PC was determined using an extinction coefficient at 342 nm equal to 42,000 M^{-1} cm^{-1} (in methanol) (Somerharju et al., 1985). The phospholipid concentration was determined by the method of Bartlett (1959).

Preparation of liposomes

Appropriate amounts of DMPC dissolved in chloroform were dried under nitrogen in Eppendorf vials. Then Pyr-PC dissolved in methanol was added into each vial at the desired mixing ratio. The mixtures were dried first under nitrogen and then under vacuum overnight. The dried mixtures were suspended in 50 mM KCl, 10^{-4} M EDTA, and 10 mM Tris at pH 7.5. The dispersion was vortexed for 2 min at $T > T_m$ to make multilamellar vesicles. The vesicles were cooled to 4°C for 30 min and then placed at 38°C for 30 min. This cooling/heating cycle was repeated 2 more times. Finally, the samples were incubated at 4°C under nitrogen for 12–24 h before fluorescence measurements. It is important to mention that cooling/heating cycles are an important step for the observation of E/M dips. Liposomes made from lipids finally dried from chloroform, instead of methanol, also exhibited E/M dips.

Large unilamellar vesicles (LUV) were prepared from multilamellar vesicles by using a lipid extruder (Lipex Biomembranes, Vancouver, BC, Canada) according to the method of Hope et al. (1985). The extrusion was operated at temperatures above the phase transition temperature, T_m, of the lipid vesicles. Polycarbonate membranes (Nuclepore, Pleasanton, CA) with varying pore sizes were used for the extrusion. The actual size of the extruded liposomes was determined by a light scattering methodology using a Coulter particle size analyzer (model N4 MD, Coulter Electronic, Hialeath, FL). The calculation was made based on the assumption that all the vesicles were spherical. The light source of the analyzer was a He-Ne laser. Detection was at an angle of 90° with respect to the excitation.

Fluorescence measurements

Fluorescence intensity measurements were made with an SLM DMX-1000 fluorometer (SLM Instruments, Urbana, IL). Samples were excited at 342 nm with 2-nm bandpath. The emission was observed through a monochromator with 4-nm bandpath. The ratio of excimer fluorescence (E) to monomer fluorescence (M) was determined using the intensities at 478 and 378 nm, respectively. The concentration of lipids used for fluorescence measurements was about 2×10^{-6} M. Fluorescence measurements under pressure were made isothermally on an SLM high pressure optical cell. The temperature of the sample was controlled by a circulating bath.

RESULTS

Effect of temperature on E/M dips

The effects of temperature on the E/M dips at two critical mole fractions, namely, 66.7 and 71.4 mol% Pyr-PC in DMPC multilamellar vesicles, have been examined. The typical results are shown in Figs. 2 and 3. Fig. 2 shows that an E/M dip at 66.7 mol% is readily observable at 31, 38, and 43°C and that the dip position remains virtually unchanged

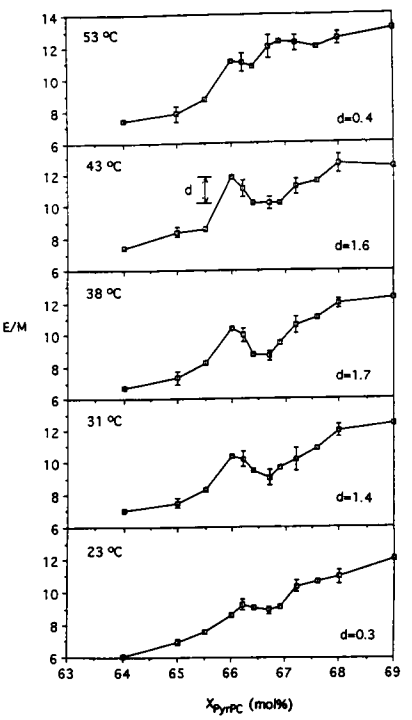

FIGURE 2 Effect of temperature on the E/M dip near the critical mole fraction 66.7 mol% Pyr-PC in DMPC multilamellar vesicles. To compare the E/M dips at different temperatures, all the samples were kept virtually at the same thermal history before fluorescence measurements. In this experiment, 12 samples with Pyr-PC mole fractions varying from 64 to 69 mol% were used for each of the five temperatures employed. Thus, vesicles at a given mixing ratio of Pyr-PC to DMPC were divided into five fractions after the vesicles had been incubated at 4°C overnight. Each fraction was then used for fluorescence measurements at one temperature only. In this way, no samples were subject to more than one temperature perturbation after they were incubated at 4°C. Typical error bars are given. The depth of the dip, d, was determined by the equation: $d = (E/M)_{max} - (E/M)_{min}$, where $(E/M)_{max}$ stands for the local maximal E/M value at $X_{PyrPC} < C_r$ and $(E/M)_{min}$ is usually the E/M value at the critical mole fraction C_r. The d values are in E/M units.

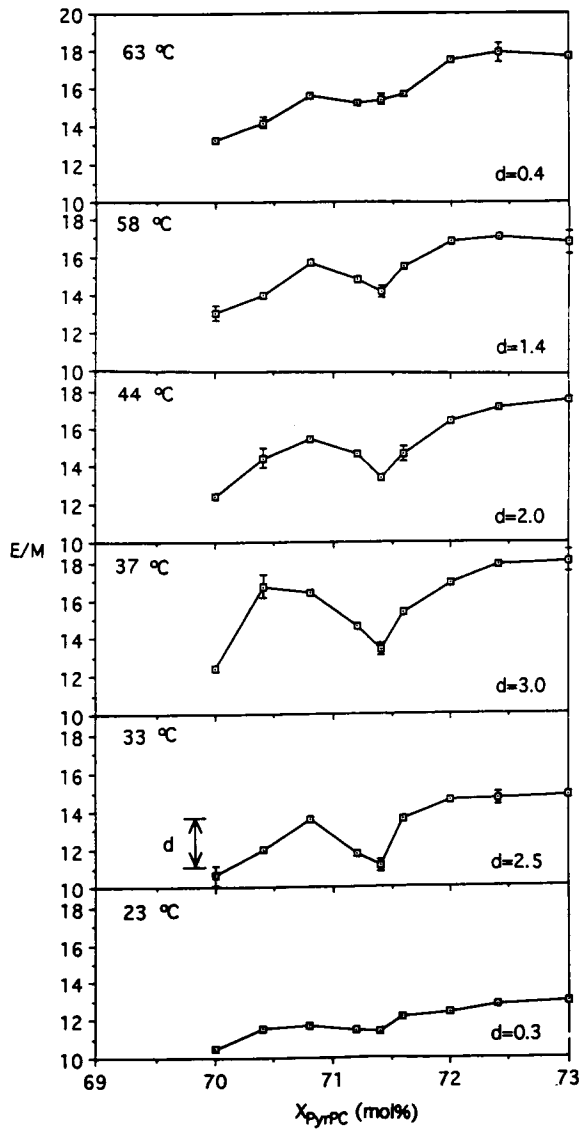

FIGURE 3 Effect of temperature on E/M dip near the critical mole fraction 71.4 mol% Pyr-PC in DMPC multilamellar vesicles. The experimental conditions are virtually the same as those described in Fig. 2.

with temperature. At 23 and 53°C, the dip is shallow, almost like a kink. The *d* values listed in Fig. 2 are the depths of the E/M dip at 66.7 mol% at the different temperatures. The *d* value was determined as follows: $d = (E/M)_{max} - (E/M)_{min}$, where $(E/M)_{min}$ is usually the E/M value at a critical Pyr-PC mole fraction C_r, and $(E/M)_{max}$ is the local maximal E/M value detected at a mole fraction slightly less than the C_r. For example, the *d* value at 43°C is calculated to be 1.62 because $(E/M)_{max}$ at 66.0 mol% = 11.85 and $(E/M)_{min} = (E/M)_{66.7\ mol\%}$ = 10.23 (Fig. 2). The *d* values between 31 and 43°C are significantly higher than those at 23 and 53°C. It should be mentioned that the above results are reproducible in a qualitative sense. For instance, from three separate experiments, it is found that the *d* value at the 66.7-mol% dip always drops at high temperatures, in the range between 53 and 60°C. The reproducibility should not be judged by the shape of the dip because it may vary with sample thermal history, a pattern typical for nonequilibrium situations. However, the position of the dip appears to be invariant from experiment to experiment.

Fig. 3 shows the typical effect of temperature on the E/M dip at the critical mole fraction 71.4 mol%. A dip at 71.4 mol% is clearly discernible at 33, 37, 44, and 58°C. At 23 and 65°C, the dip is much smaller. The depths (*d*) of the 71.4 mol% dip at various temperatures are listed in Fig. 3. The maximal depth is at 37°C; thereafter, the *d* value begins to drop. The depth decreases to near the basal value at 63°C.

Fig. 4 *A–D* show the temperature dependence of E/M at various Pyr-PC/DMPC mixing ratios in the temperature range 5–50°C. Between 5 and 35 mol% Pyr-PC, E/M initially increases with increasing temperature, followed by a steady decrease up to 25–30°C, and then E/M increases again with temperature (Fig. 4, *A* and *B*). This trend forms an N-shaped curve. At 47–52 mol% Pyr-PC, the N shape is less noticeable (Fig. 4 *C*). At 65 mol% or higher, the curve becomes biphasic (Fig. 4 *D*). Evidently, the variation of E/M with temperature is dependent upon the mole fraction of Pyr-PC.

Effect of vesicle diameter on E/M dips

The effect of vesicle size on the E/M dip at 66.7 mol% Pyr-PC at 38°C is illustrated in Fig. 5. Columns A and B are two independent experiments; yet, both show similar results. The E/M dip at 66.7 mol% remains discernible when the membrane is converted from multilamellar to large unilamellar structures. However, the depth of the E/M dip (*d*) decreases with decreasing the vesicle size. When the average diameter of the vesicle (*r*) is reduced to about 64 nm, the dip becomes shallow and split. It is also noticed that, despite a larger diameter for multilamellar vesicles, the depth of multilamellar vesicles is less than that of large unilamellar vesicles (e.g., r = 396–576 nm). This is probably because multilamellar vesicles have a more heterogeneous size distribution.

Effect of pressure on E/M dips

Fig. 6 shows the effects of pressure on E/M dips in Pyr-PC/DMPC multilamellar vesicles at 30°C. E/M dips are clearly discernible at 28.6, 33.3, 50, and 66.7 mol% Pyr-PC (Fig. 6 *A–D*) at the pressure range 0.001–0.7 kbar. At much higher pressures, the dips are not detected. The dip positions agree with the critical mole fractions *Y* or *Y'* predicted from Eqs. 1 and 2. At 30°C and at pressures below 0.7 kbar, pure DMPC should be in the liquid-crystalline state according to the phase diagram constructed by Winter and Pilgrim (1989). Although the temperature-pressure phase diagram of Pyr-PC/DMPC mixtures is not available at the present time, it can be postulated that Pyr-PC is likely to lower the T_m of the DMPC molecules because pure Pyr-PC has a phase transition temperature (14.5°C; Somerharju et al., 1985) that is lower than that of pure DMPC (24°C). This suggests that at 30°C and at pressures below 0.7 kbar, Pyr-PC/DMPC is most

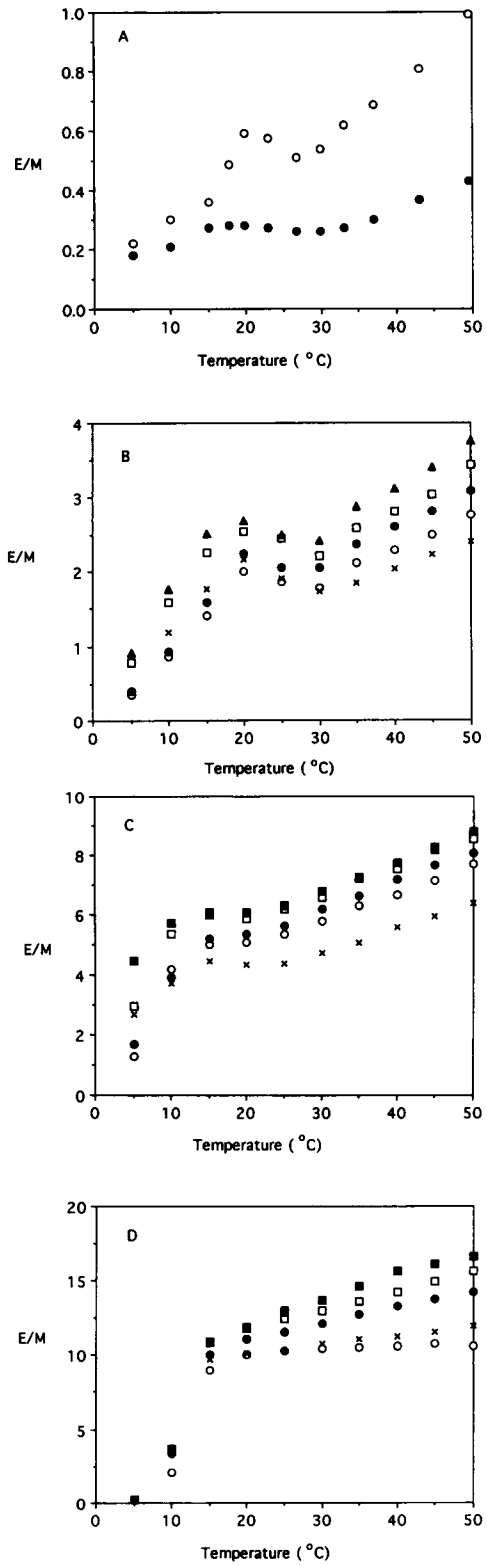

FIGURE 4 Effect of temperature on the E/M at various Pyr-PC mole fractions in DMPC multilamellar vesicles. E/M was measured as a function of temperature in the ascending mode at a scanning rate of 24–36°/h. Pyr-PC mole fractions are: (*A*) 5 mol% (●) and 10 mol% (○); (*B*) 32.2 mol% (○), 32.6 mol% (●), 33.3 mol% (×), 34.0 mol% (□) and 34.8 mol% (■); (*C*) 47.0 mol% (○), 48.0 mol% (●), 50.0 mol% (×), 51.0 mol% (□), and 52.0 (■); (*D*) 65.4 mol% (○), 65.8 mol% (●), 66.7 mol% (×), 67.2 mol% (□), and 67.6 mol% (■).

likely to be in the liquid-crystalline state. Hence, it can be suggested from Fig. 6 that the E/M dips persist as long as the membrane is in the liquid-crystalline state.

Fig. 7 *A* shows the effects of pressure on the E/M values of Pyr-PC in DMPC multilamellar vesicles at 30°C. E/M undergoes an abrupt decrease at elevated pressures with a 50% change in E/M at about 1.1 kbar. The abrupt decrease in E/M shown in Fig. 7 *A* is believed to be due to the pressure-induced phase transition from the liquid-crystalline state to the gel state. It is clear from Fig. 7 *A* that, at pressures below 0.7 kbar, the slope of E/M versus pressure at noncritical mole fractions (e.g., 48, 49, 52, 53 mol%) is significantly greater than that at the critical mole fraction (i.e., 50 mol%).

A similar pattern is seen in the case of Pyr-PC/DMPC mixtures in the neighborhood of 33.3 mol% (Fig. 7 *B*). An abrupt decrease in E/M occurs between 0.6 and 1.2 kbar. Below 0.5 kbar, E/M decreases steadily with increasing pressure at noncritical mole fractions (e.g., 31, 32, 35, 36 mol%); within the same pressure range, E/M increases slightly with pressure.

The reproducibility of the E/M value requires some comment. First, the system is in nonequilibrium situations. Second, the E/M value depends on the lateral organization of Pyr-PC, especially the arrangement of the nearest neighbors around a Pyr-PC molecule in the irregular region. The lateral arrangement of Pyr-PC varies with the thermal history of the sample. It is difficult to reproduce exactly the same thermal history from separate sample preparations. This explains why the E/M values from two independent preparations are quite different (Figs. 5–7). However, when vesicles were kept virtually at the same thermal history, they showed very similar E/M values (Figs. 2 and 3). Thus, it is immaterial to address the reproducibility of the E/M value from two independent preparations (e.g., *A* and *B* in Fig. 5 and the data in Fig. 6 versus the data in Fig. 7). What is important is that the dips occur at the expected critical mole fractions and that the effects of temperature, pressure, and radius of curvature are qualitatively reproducible.

DISCUSSION

The physical meaning of the depth of the dip can be understood based on a concept developed from computer simulations (Sugar et al., 1993, 1994). Computer simulations suggest that lipid regular distribution and irregular distribution coexist and that the ratio of regular areas to irregular areas (Z) reaches a local maximum at critical concentrations and a local minimum between two adjacent critical concentrations. In the case of 66.7 mol% Pyr-PC in DMPC, Pyr-PC molecules in the regular regions are maximally separated into hexagonal super-lattices (Fig. 1, *top*). Thus, in the regular region, only unlabeled acyl chains can be found in the nearest neighbors of a pyrene-containing acyl chain. The pyrene moieties in the regular regions (Fig. 1, *top*) are not expected to make any appreciable contributions to excimer fluorescence. Excimer fluorescence should come exclusively from the irregular regions where two pyrene-containing acyl

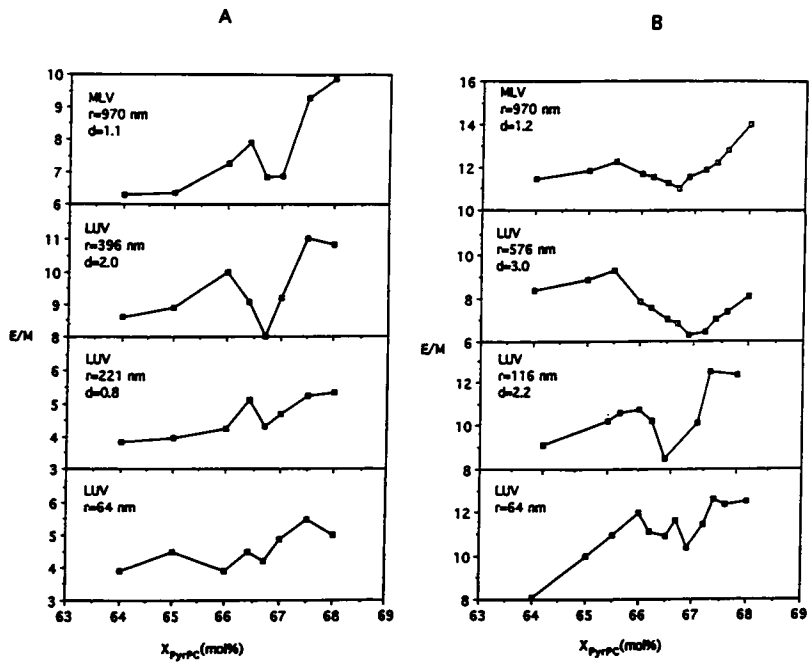

FIGURE 5 Effect of vesicle diameter on the depth of E/M dips near the critical mole fraction 66.7 mol% Pyr-PC in DMPC. r is the average diameter of the vesicles determined from light scattering as described in Materials and Methods. d is the depth of the E/M dip determined using the method described in Fig. 2. The temperature for fluorescence measurements was 38°C. Columns A and B represent two independent experiments. MLV at a given mixing ratio of Pyr-PC to DMPC were divided into three fractions after the vesicles had been incubated at 4°C overnight. Each fraction was then passed through the lipid extruder at 35°C using the desired filter pore size. The obtained unilamellar vesicles were incubated at 4°C overnight before fluorescence measurements.

chains may be nearest neighbors. Also, regular regions, such as the one depicted in Fig. 1 (*top*), require a stringent structural arrangement where membrane defect or void space is not preferred. In contrast, in the irregular regions, membrane defect is more likely to occur; membrane defect creates free volume, which facilitates lipid lateral diffusion (Galla et al., 1979; Vaz and Hallmann, 1983; Peters and Beck, 1983; Muller and Galla, 1983; Vaz et al., 1985; King and Marsh, 1986; Muller and Galla, 1987). Lateral diffusion brings about collisions between pyrene moieties and, thus, an increased E/M (Birks et al., 1963). By considering nearest neighbors (local concentration) and lipid lateral diffusion, it becomes clear that irregular regions should generate most, if not all, of the excimers. Because the ratio of regular areas to irregular areas (Z) reaches a local maximum at critical concentrations and a local minimum between two adjacent critical concentrations (Sugar et al., 1993, 1994), E/M should drop to a local minimum at critical mole fractions (either Y_{PyrPC} or Y'_{PyrPC}) and reaches a local maximum between two neighboring critical mole fractions. This explains why the E/M dips are observed at critical Pyr-PC mole fractions. It also follows that the depth of the E/M dip should be a useful index reflecting how sharply the ratio of regular areas to irregular areas (Z) varies from a concentration lower than the critical mole fraction C_r to a concentration higher than C_r. If there is a dramatic change in lipid lateral organization between a critical mole fraction and its neighboring noncritical mole fractions, a sharp change in Z would occur and a pronounced dip in the plot of E/M versus Pyr-PC mole fraction should be observed. Conversely, if there is no significant change in the lateral organization in the vicinity of a critical mole fraction C_r, no discernible E/M dips would be observed. In fact, according to Monte Carlo simulations (Sugar et al., 1994), an E/M kink is obtained at a critical concentration when the pyrene-labeled acyl chains are regularly arranged within several disconnected areas of the membrane, whereas in the case of E/M dips, a connected area of regularly arranged pyrene-labeled acyl chains percolates through the whole membrane.

As shown in Figs. 2 and 3, an E/M dip is discernible at moderate temperatures and becomes a kink at higher temperatures. This observation implies that, at moderate temperatures, there is a distinct difference in lateral organization between critical mole fractions and noncritical mole fractions. This difference diminishes at high temperatures. This effect is not unexpected because the existence of an E/M dip relies on the balance between the energy minimization due to the maximal separation (a self-ordered phenomenon) of the bulky pyrene rings and the entropy-driven randomization (Tang and Chong, 1992). This balance should break down at high temperatures where the entropy-driven randomization prevails. The number of structural defects in self-ordered systems usually increases with increasing thermal fluctuations; for example, the magnetism becomes zero when the temperature is raised to the Curie point of ferromagnets (Haken, 1983). At high temperatures, thermal fluctuations will eventually lead to a transition in lipid lateral organization from regular (ordered) to random (disordered) distributions. It should be mentioned that temperature elevation increases the cross sectional area of the host as well as the guest membrane lipids. If thermal expansivities for both DMPC and Pyr-PC are similar, then pyrene-labeled acyl chains may remain bulky relative to the unlabeled acyl chains at $T > T_m$. As a result, lattice deformation by pyrene moiety and the repulsive interaction between pyrene-containing acyl chains persist even at elevated temperatures.

The N-shaped curve in the plot of E/M versus temperature (Fig. 4, A and B) was previously reported in pyrene/DPPC (Galla and Sackmann, 1974; Muller and Galla, 1983),

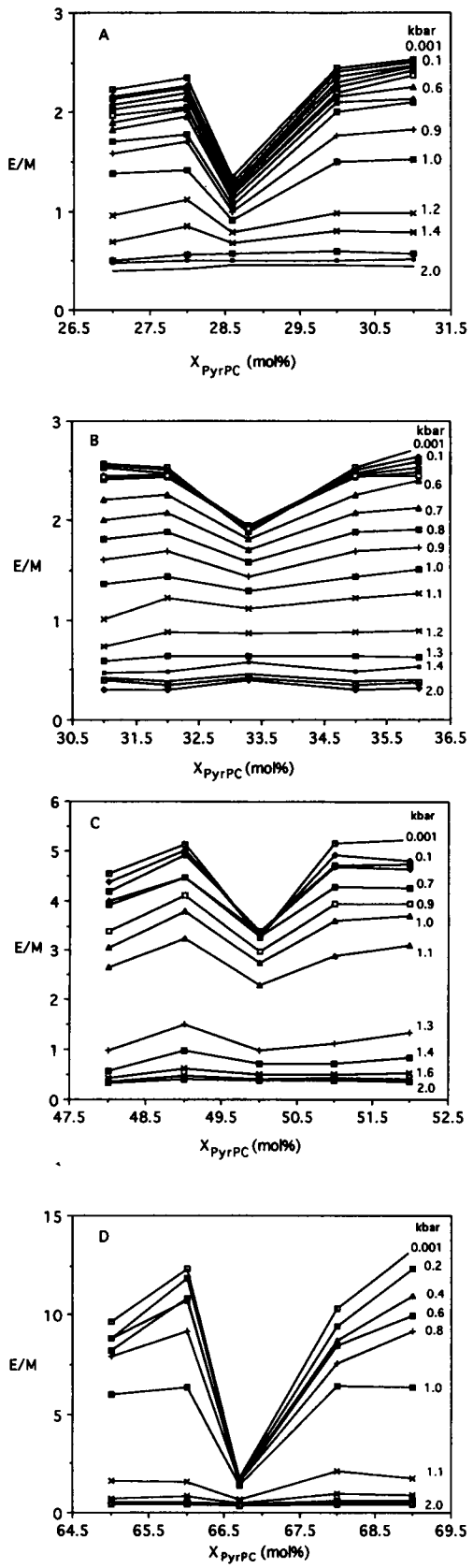

FIGURE 6 Effect of pressure on E/M dips for Pyr-PC/DMPC multilamellar vesicles in the neighborhood of critical Pyr-PC mole fractions: (*A*)28.6 mol%, (*B*) 33.3 mol%, (*C*) 50 mol%, and (*D*) 66.7 mol%. Temperature = 30°C.

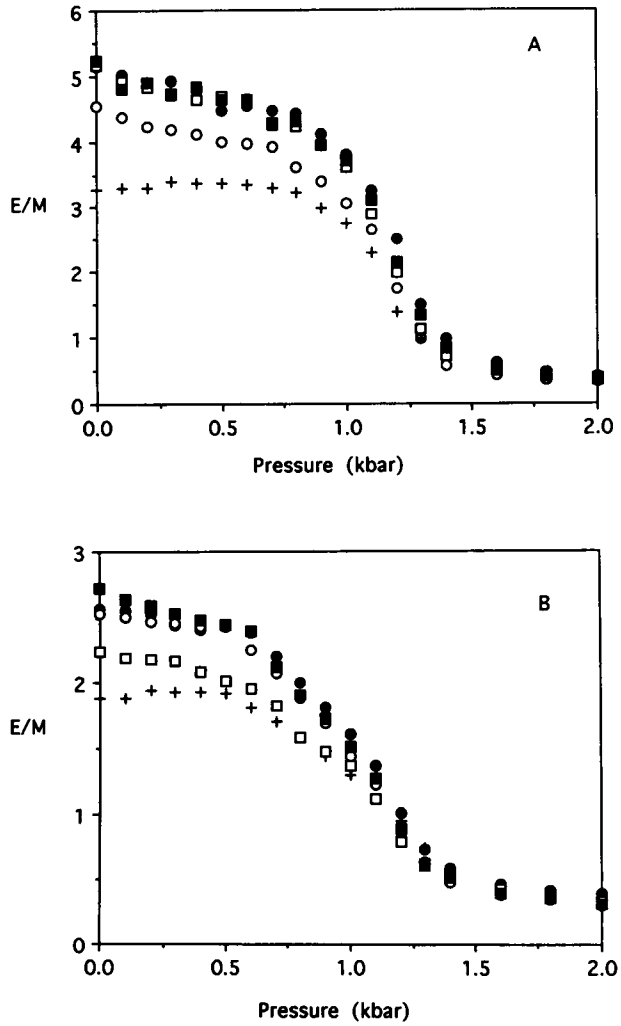

FIGURE 7 (*A*) Effect of pressure on E/M in Pyr-PC/DMPC multilamellar vesicles at 30°C. Mol% Pyr-PC: 48 (○), 49 (●), 50 (+), 52 (□), and 53 (■). (*B*) Effect of pressure on E/M in Pyr-PC/DMPC multilamellar vesicles at 30°C. Mol% Pyr-PC: 31 (○), 32 (●), 33.3 (+), 35 (□), 36 (■).

Pyr-PC/DPPC (Somerharju et al., 1985; Hresko et al., 1986; Viani et al., 1988) and *N*-pyrene-dodecanoyl sulfatides/DPPC mixtures (Viani et al., 1988). However, Hresko et al. (1986) observed the N-shaped curve only in the mixtures of Pyr-PC/DPPC, not in Pyr-PC/DMPC. Their explanation was that Pyr-PC preferred the fluid phase in the two-phase mixing region in Pyr-PC/DMPC mixtures, whereas Pyr-PC partitioned equally into the two phases in the two-phase region in Pyr-PC/DMPC mixtures. In contrast to their results, we observe the N-shaped curve in Pyr-PC/DMPC mixtures over a wide range of concentrations (Fig. 4, *A* and *B*). The reason for the discrepancy between our results and the results of Hresko et al. (1986) is not clear, but certainly is not due to the cooling/heating cycles or to the low temperature incubation period employed in the sample preparation (data not shown).

The entire N-shaped curve can be divided into three regions: I, II, and III, as depicted in Fig. 8. Region II is the middle section of the N-shaped curve, which is believed to

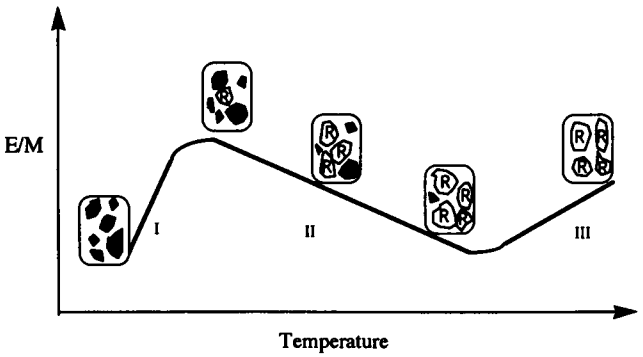

FIGURE 8 Schematic description of the molecular mechanism responsible for the N-shaped curve observed in Pyr-PC/PC mixtures. The areas labeled R are designated as regular distribution areas. The black areas represent Pyr-PC clusters. The blank areas in each square are irregular areas where no regular patterns can be recognized. Each square represents the membrane at a different physical state.

reflect the gel-to-liquid-crystalline phase transition (Galla and Sackmann, 1974). Accordingly, Region I and Region III can be assigned to the gel and the liquid-crystalline state, respectively. Collision frequency of pyrene moieties should increase with increasing temperature (Birks et al., 1963; Galla and Sackmann, 1974); thus E/M should increase with increasing temperature. In this regard, the behavior of E/M in Region II (Figs. 4 and 8) is abnormal. Galla and Sackmann (1974) explained the anomalous decrease in E/M during the phase transition as a result of forming pyrene clusters in the gel phase of the lipid matrix. Viani et al. (1988) attributed the anomaly to the lateral re-distribution of Pyr-PC molecules. They suggested that above the T_m of DPPC, Pyr-PC is evenly distributed. As the temperature is decreased, Pyr-PC molecules are excluded into fluid domains. The increase in the surface density of Pyr-PC in the fluid domains leads to increased jumping frequency of Pyr-PC, and consequently increased E/M with decreasing temperature.

Based on our previous studies (Tang and Chong, 1992; Sugar et al., 1993, 1994) and the results shown in this study, we herein propose a simple explanation for the N-shaped curve in the plot of E/M versus temperature. It can be suggested that regular distribution (labeled R in Fig. 8) and irregular distribution (the blank area in Fig. 8) coexist in Region III. In Region I, regular distribution is unlikely to occur because E/M dips are not readily observable in the gel phase (for example, membranes at high pressures, Fig. 6). This leaves only two possibilities (Von Dreele, 1978) for lipids in the gel phase (Region I), that is, domain segregation or random distribution. If Pyr-PC molecules are randomly distributed in the gel phase, the increasing rate of E/M with temperature in Region I should be less than that in Region III (the liquid crystalline state), because the lateral diffusion rate of lipids in the gel phase is known to be very much limited, as compared to that in the liquid crystalline state. However, the results in Fig. 4, *A* and *B* show that the increasing rate of E/M with temperature in Region I is even higher than that in Region III. This argues against random distribution in Region I. To this end, it may be proposed that Pyr-PC clusters are formed in the gel phase of Pyr-PC/DMPC mixtures (Region I in Fig. 8). In the Pyr-PC clusters, slight changes in lateral motion or pyrene ring orientation (Sugar et al., 1991) can greatly enhance excimer formation due to the close proximity of Pyr-PC molecules.

The decrease of the E/M value in the middle region (Region II in Fig. 8) of the N-shaped curve can now be understood in terms of the conversion from the Pyr-PC clusters to the regular distributions. As the temperature is increased from the beginning point to the end point of Region II, more and more Pyr-PC clusters are melted and Pyr-PC molecules become maximally separated as a result of regular distribution. This change in lateral organization explains why E/M decreases with increasing temperature in Region II. As the phase transition is completed, the E/M value decreases to a minimal value. At that point, the lateral organization is composed of both regular and irregular areas. Thereafter, a rise in temperature increases the lateral diffusion of Pyr-PC in the irregular areas, which gives rise to an increase in the collisional frequency between pyrene monomers, thus, an increase in E/M. It is important to mention that although regular regions and irregular regions coexist, they are not static. Lipids in regular and irregular regions undergo constant exchanges. Hence, the schematic description of lipid lateral organization at each stage shown in Fig. 8 should be viewed as an instant lateral arrangement that has a dynamic nature. Furthermore, it has been argued before that the presence of regular distribution contradicts the random nature of lipid lateral diffusion. According to the above discussion, this argument is unnecessary because random lipid lateral diffusion is allowed only in the irregular regions, not in the regular regions.

The pressure data in the liquid-crystalline state (<0.7 kbar at 30°C) exhibit a sharp contrast between membranes at critical mole fractions (33.3 and 50 mol%) and noncritical mole fractions. At noncritical Pyr-PC mole fractions, E/M initially decreases steadily with increasing pressure, then decreases abruptly. In contrast, at critical mole fractions, E/M changes little with pressure before the abrupt decrease in E/M occurs. The steady decrease in E/M with pressure observed at noncritical mole fractions below 0.7 kbar is not surprising because similar results have been previously reported in various membrane systems (Flamm et al., 1982; Muller and Galla, 1983, 1987; Turley and Offen, 1985, 1986; Macdonald et al., 1988; Kao et al., 1992). In those studies, the decrease in E/M with pressure was interpreted in terms of a pressure-induced decrease in membrane fluidity or membrane free volume, which in turn gives rise to a decreased lateral diffusion. Note that the lateral diffusion of lipids in membranes has been shown (Galla et al., 1979; Vaz and Hallman, 1983; Peters and Beck, 1983; Vaz et al., 1985; King and Marsh, 1986) to follow the free volume model (Cohen and Turnbull, 1959) in a manner similar to a solute molecule in liquids.

The striking observation from Fig. 7, *A* and *B* is that the pressure dependence of E/M at critical mole fractions is distinctly different from that at noncritical mole fractions. This difference can be understood in terms of changes in lipid lateral organization from a noncritical to a critical mole fraction. Under isothermal conditions, pressure produces only volume changes. Previous studies have shown that increased pressure reduces membrane volume in the liquid-crystalline state of lipid bilayers (Liu and Kay, 1977; Tosh and Collings, 1986). This decrease in volume should cause two effects on Pyr-PC/DMPC systems: (i) pressure reduces the lateral diffusion of lipids, thus decreasing the E/M value, and (ii) pressure shortens the intermolecular distance, thus increasing the E/M value. At critical mole fractions, membranes possess less free volume as a result of a higher ratio of regular area to irregular area. In this case, the negative contribution from factor (i) may be offset by the positive contribution from factor (ii) such that E/M changes very little with pressure (50 mol% Pyr-PC in Fig. 7 *A* and 33.3 mol% Pyr-PC in Fig. 7 *B* at pressures below 0.7 kbar). At noncritical mole fractions, membranes possess more free volume because of a higher ratio of irregular to regular area. In this case, factor (i) would be dominating and, consequently, E/M decreases steadily with increasing pressure.

In the pressure range 0.001–0.7 kbar, the E/M dips remain discernible, the depth of the dip decreases only slightly with increasing pressure, and the dip position remains virtually unchanged (Fig. 6). These results suggest that lipid regular distribution persists in this pressure range.

Within the liquid-crystalline state of lipid bilayers, the variation of lipid intermolecular distance by temperature and pressure is rather limited. The importance of intermolecular distance between Pyr-PC molecules on the E/M dip, thus, on the regular distribution, can be better demonstrated by varying the radius of curvature of the vesicle. When the radius of curvature is small, lipid headgroups in the outer monolayer are more separated and pyrene-labeled acyl chains are able to fit better into the membrane lattice. In this situation, the elastic deformation of the membrane lattice around each pyrene-labeled acyl chain decreases and the long-range repulsive interaction between the labeled chains becomes weaker. This explains why the depth of the E/M dip at 66.7 mol% Pyr-PC becomes shallow when the radius of curvature is small (e.g., r = 64 nm in Fig. 5). In addition, when the vesicle diameter is small (e.g., 64 nm), the lipids in the outer and inner monolayers experience different constraints. This may cause a heterogeneous distribution of Pyr-PC between the two monolayers. As a result, the actual Pyr-PC mole fraction in each monolayer may deviate from the apparent mole fraction, leading to a split dip (r = 64 nm in Fig. 5).

In conclusion, the effects of vesicle diameter, pressure, and temperature on the E/M dips all agree qualitatively with theoretical predictions and with the concept of lipid regular distribution. Several physical principles underlying lipid regular distribution are revealed, which are summarized as follows.

(i) In the liquid crystalline state of Pyr-PC/DMPC mixtures, regular and irregular regions coexist. Lipid lateral diffusion takes place virtually exclusively in the irregular areas where membrane defects are available. Note that lateral diffusion of pyrene-labeled acyl chains and regular areas are mutually exclusive. This implies that the ordered lipid regular distribution and random lipid lateral diffusion may occur at the same time but at different places of the membrane.

(ii) The E/M dip is significantly reduced when the radius of curvature of the membrane becomes small. This result agrees with the idea that E/M dips and the regular distribution of the pyrene-labeled acyl chains are caused by the long-range repulsive interaction between the labeled chains. The repulsive interaction results from the elastic lattice deformation around the bulky pyrene moiety. When the radius of curvature becomes small, pyrene-containing acyl chains are able to fit better into the membrane lattice and the elastic deformation decreases.

(iii) The presence of E/M dips requires a fine balance between the free energy minimization due to the maximal separation of the bulky pyrene rings and the entropy-driven randomization. When the temperature is raised, the number of structural defects increases and the regular areas are reduced. E/M dips will diminish at high temperatures where thermal fluctuation dominates or entropy-driven randomization prevails.

(iv) E/M dips seem to respond to the perturbations of pressure and temperature according to lipid phase behavior. E/M dips appear favorably in the liquid-crystalline state of the matrix lipid. In the gel phase, dips are rarely seen. This suggests that E/M dips are a lipid-involving phenomenon, rather than an artifact of fluorescence measurements.

(v) Pressure data suggest that membrane free volume is less abundant at critical Pyr-PC mole fractions than at noncritical mole fractions. This indicates that membrane free volume varies with Pyr-PC mole fraction in a periodic manner because there are many critical mole fractions over a wide range of Pyr-PC concentrations. This result is in parallel with the results obtained from computer simulations that indicate that the ratio of regular region to irregular region reaches a local maximum at critical Pyr-PC mole fractions and a local minimum between two neighboring critical mole fractions.

Although our system of study is a simple and artificial one, the physical principles that describe our model system can be generally applied to real biological membranes because Pyr-PC-like bulky molecules (e.g., cholesterol) relative to bilayer phospholipids do exist in biological membranes. The occurrence of regular distribution in the liquid-crystalline state is of biological significance because most biomembrane lipids are in the fluid state at physiological conditions. Among all the physical principles revealed above, the periodic variation of membrane volume with Pyr-PC mole fraction is by far the most important because many membrane events such as lipid lateral diffusion (Galla et al., 1979; Vaz and Hallman, 1983; Peters and Beck, 1983; Vaz et al., 1985; King and Marsh,

1986), membrane fusion (Hui et al., 1981), and lipid spontaneous transfer between membranes (Wimley and Thompson, 1991) have been previously suggested to be closely related to membrane free volume or membrane defect.

This research was supported in part by the U. S. Army Research Office and National Science Foundation–Minority Research Center of Excellence (RII-8714805).

REFERENCES

Bartlett, G. R. 1959. Phosphorus assay in column chromatography. *J. Biol. Chem.* 234:466–468.

Birks, J. B., D. J. Dyson, and I. H. Munro. 1963. Excimer fluorescence. II. Lifetime studies of pyrene solutions. *Proc. R. Soc. Lond. A.* 275: 575–588.

Cohen, M. H., and D. Turnbull. 1959. Molecular transport in liquid and glasses. *J. Chem. Phys.* 31:1164–1169.

Flamm, M., T. Okubo, N. J. Turro, and D. Schachter. 1982. Pressure dependence of pyrene excimer fluorescence in human erythrocyte membranes. *Biochim. Biophys. Acta.* 687:101–104.

Galla, H.-J., and E. Hartmann. 1980. Excimer-forming lipids in membrane research. *Chem. Phys. Lipids.* 27:199–219.

Galla, H.-J., W. Hartmann, U. Theilen, and E. Sackmann. 1979. On two-dimensional passive random walk in lipid bilayers and fluid pathways in biomembranes. *J. Membr. Biol.* 48:215–236.

Galla, H.-J., and E. Sackmann. 1974. Lateral diffusion in the hydrophobic region of membranes: use of pyrene excimers as optical probes. *Biochim. Biophys. Acta.* 339:103–115.

Haken, H. 1983. Synergetics: Nonequilibrium Phase Transition and Self-Organization. Springer-Verlag, Berlin. p. 3.

Hui, S. W., T. P. Stewart, and L. T. Boni. 1981. Membrane fusion through point defects in bilayers. *Science.* 212:921–923.

Hope, M. J., M. B. Bally, G. Webb, and P. R. Cullis. 1985. Production of large unilamellar vesicles by a rapid extrusion procedure. Characterization of size distribution, trapped volume and ability to maintain a membrane potential. *Biochim. Biophys. Acta.* 812:55–65.

Hresko, R. C., I. P. Sugar, Y. Barenholz, and T. E. Thompson. 1986. Lateral distribution of a pyrene-labeled phosphatidylcholine in phosphatidylcholine bilayers: fluorescence phase and modulation study. *Biochemistry.* 25:3813–3823.

Kao, Y. L., E. L. Chang, and P. L.-G. Chong. 1992. Unusual pressure dependence of the lateral motion of pyrene-labeled phosphatidylcholine in bipolar lipid vesicles. *Biochem. Biophys. Res. Commun.* 188: 1241–1246.

King, M. D., and D. Marsh. 1986. Free volume model for lipid lateral diffusion coefficients. Assessment of the temperature dependence in phosphatidylcholine and phosphatidylethanolamine bilayers. *Biochim. Biophys. Acta.* 862:231–234.

Kinnunen, P. K. J., A. Tulkki, H. Lemmetyinen, J. Paakkola, and A. Virtanen. 1987. Characteristics of excimer formation in Langmuir-Blodgett assemblies of 1-palmitoyl-2-pyrenedecanoylphosphatidylcholine and dipalmitoylphosphatidylcholine. *Chem. Phys. Lett.* 136: 539–545.

Liu, N.-I., and R. L. Kay. 1977. Redetermination of the pressure dependence of the lipid bilayer phase transition. *Biochemistry.* 16:3484–3486.

Macdonald, A. G., K. W. J. Wahle, A. R. Cossins, and M. K. Behan. 1988. Temperature, pressure and cholesterol effects on bilayer fluidity; a comparison of pyrene excimer/monomer ratios with the steady-state fluorescence polarization of diphenylhexatriene in liposomes and microsomes. *Biochim. Biophys. Acta.* 938:231–242.

Muller, H.-J., and H.-J. Galla. 1983. Pressure variation of the lateral diffusion in lipid bilayer membranes. *Biochim. Biophys. Acta.* 733:291–294.

Muller, H.-J., and H.-J. Galla. 1987. Chain length and pressure dependence of lipid translational diffusion. *Eur. J. Biophys.* 14:485–491.

Mustonen, P., J. A. Virtanen, P. J. Somerharju, and P. K. J. Kinnunen. 1987. Binding of cytochrome c to liposomes as revealed by the quenching of fluorescence from pyrene-labeled phospholipids. *Biochemistry.* 26: 2991–2997.

Peters, R., and K. Beck. 1983. Translational diffusion in phospholipid monolayers measured by fluorescence microphotolysis. *Proc. Natl. Acad. Sci. USA.* 80:7183–7187.

Ruocco, M. J., and G. G. Shipley. 1982. Characterization of the subtransition of hydrated dipalmitoyl phosphocholine bilayers. Kinetics, hydration and structural studies. *Biochim. Biophys. Acta.* 691:309–320.

Somerharju, P. J., J. A. Virtanen, K. K. Eklund, P. Vainio, and P. K. J. Kinnunen. 1985. 1-Palmitoyl-2-pyrenedecanoyl glycerophospholipids as membrane probes: evidence for regular distribution in liquid-crystalline phosphatidylcholine bilayers. *Biochemistry.* 24:2773–2781.

Sugar, I. P., D. Tang, and P. L.-G. Chong. 1993. Use of Monte Carlo simulations to study lateral organization of lipids in Pyr-PC/DMPC membranes. *Biophys. J.* 64:A74.

Sugar, I. P., D. Tang, and P. L.-G. Chong. 1994. Monte Carlo simulation of lateral distribution of molecules in a two-component membrane. Effect of long-range repulsive interactions. *J. Phys. Chem.* In press.

Sugar, I. P., J. Zeng, and P. L.-G. Chong. 1991. Use of Fourier transforms in the analysis of fluorescence data. 3. Fluorescence of pyrene-labeled phosphatidylcholine in lipid bilayer membrane. A three-state model. *J. Phys. Chem.* 95:7524–7534.

Tang, D., and P. L.-G. Chong. 1992. E/M dips: evidence for lipids regularly distributed into hexagonal super-lattices in pyrene-PC/DMPC binary mixtures at specific concentrations. *Biophys. J.* 63:903–910.

Tosh, R. E., and P. J. Collings. 1986. High pressure volumetric measurements in dipalmitoylphosphatidylcholine bilayers. *Biochim. Biophys. Acta.* 859:10–14.

Turley, W. D., and H. W. Offen. 1985. Fluorescence detection of gel-gel phase transitions in DMPC vesicles at high pressures. *J. Phys. Chem.* 89:3962–3964.

Turley, W. D., and H. W. Offen. 1986. Lipid microviscosity of DMPC vesicles at high pressures. Dipyrenylpropane excimer fluorescence. *J. Phys. Chem.* 90:1967–1970.

Vaz, W. L. C., R. M. Clegg, and D. Hallmann. 1985. Translational diffusion of lipids in liquid crystalline phase phosphatidylcholine multilayers. A comparison of experiment with theory. *Biochemistry.* 24:781–786.

Vaz, W. L. C., and D. Hallman. 1983. Experimental evidence against the applicability of the Saffman-Delbruck model to the translational diffusion of lipids in phosphatidylcholine bilayer membranes. *FEBS Lett.* 152: 287–290.

Viani, P., C. Galimberti, S. Marchesini, G. Cervato, and B. Cestaro. 1988. N-Pyrene dodecanoyl sulfatide as membrane probe: a study of glycolipid dynamic behavior in model membranes. *Chem. Phys. Lipids.* 46:89–97.

Virtanen, J. A., P. Somerharju, and P. K. J. Kinnunen. 1988. Prediction of patterns for the regular distribution of soluted guest molecules in liquid crystalline phospholipid membranes. *J. Mol. Electr.* 4:233–236.

Von Dreele, P. H. 1978. Estimation of lateral species separation from phase transitions in nonideal two-dimensional lipid mixtures. *Biochemistry.* 17: 3939–3943.

Wimley, W. C., and T. E. Thompson. 1991. Transbilayer and interbilayer phospholipid exchange in dimyristoylphosphatidylcholine/dimyristoylphosphatidylethanolamine large unilamellar vesicles. *Biochemistry.* 30: 1702–1709.

Winter, R., and W.-C. Pilgrim. 1989. A SANS study of high pressure phase transitions in model biomembranes. *Ber. Bunsenges. Phys. Chem.* 93: 708–717.